Peristaltic transport of micropolar fluid through porous medium in a symmetric channel with heat and mass transfer in the presence of generation and radiation

S.Sridhar [1], V. Ramesh Babu[2]
[1]Research Scholar, Rayalaseema University, Kurnool, A.P. India
[2]Department of Mathematics, Rashtriya Sanskrit Vidyapeetha, Central Deemed University, Tirupati, A.P., India

Abstract:

We investigated the effects of heat generation and radiation on convective heat and mass transfer electrically conducting micropolar fluid through porous medium in a symmetric channel. The velocity, temperature and concentration have been evaluated for different parametric variations. The pressure drop and friction force have been calculated for difference variations. The rate of heat and mass transfer on the wall have been numerically evaluated.

Keywords: Micropolar fluid, porous medium, presence of generation and radiation

1. INTRODUCTION

Peristalsis is defined as a wave of relaxation contraction (expansion) imparted by the walls of a flexible conduit, thereby pumping the enclosed material, it is a nature's way of moving the content within hollow muscular structures by successive contraction of their muscular fibers (Eytan et al., [16]; Fung and Yih, [17]; Mishra and Rao, [30]; Mekheimer, [28]. Peristalsis is now well-known to the physiologists to be one of the major mechanisms for fluid transport in many biological systems, as it results physiologically from neuron muscular properties of the tubular smooth muscles (Srivastava and Srivastava, [41]; El-Shehawey et al., [13]; Gharsseldien et al., [19]; Gharsseldien, [18]).

The peristaltic transport may be involved in many biological organs, for instance, moving food through the esophagus; movement of chime in the gastrointestinal tract; urine transport from the kidney to the bladder through the ureter; transport of spermatozoa in the ducts efferents of male reproduction tract and in the cervical canal of the female; movement of ova in the fallopian tub; vasomotion of small blood vessels such as venules and capillaries as well as blood flow in arteries, and in many other glandular ducts (El-Shehawey et al., [13]; El- Shehawey and Husseny, [14]; Mekheimer, [28]; Hayat [22]; Mishra and Rao, [30]; Srivastava and Srivastava, [41]; Bayada and Banhaoucha [6]). There are also many industrial applications of the peristaltic transport like, blood pumps in heart lung machine, transport of corrosive fluid, where the contact of the fluid with the machinery parts is prohibited (Mishra and Rao, [30]).

The theory of microfluid introduced by Eringen, deals with a class of fluids which exhibit certain microscopic effects arising from the local structure and micro-motions of the fluid elements. A subclass of these fluids is the micropolar fluids, like blood, liquid crystals and polymers, can support couple stresses, body couples and exhibit micro-rotational and micro-inertial effects. Eringen is the first researcher who put out the theory to find a mathematical model of the micropolar fluids (Eringen, [15]). These equations are a

generalization of the (Newtonian) Navier-Stokes equations and deals with three fields: velocity vector V, the pressure of the fluid P and microrotation vector, together with some viscosity parameters and material constants to describe the behavior of the fluid (Eldabe et al., [11] and El-Sayed et al., [12]). Some researchers attempted studying the peristaltic flow problems concerning the micropolar fluids, (Ali and Hayat [2]; Devi and Devanathan, [7]; Hayat and Ali, [20]; Mekheimer and Abd Elmaboud, [29]; Muthu et al., [31,32]; Srinivasacharya et al., [40]) and others studied the heat transfer effect with peristalsis or not for different fluids (Abo-Eldahab et al. [1]; Eldabe, [8]; Eldabe et al., [9]; Eldabe and Mohamed, [10]; El-Sayed et al., [12]; Hayat and Hina, [23]; Nadeem and Noreen [35]; Nadeem et al., [36]).

Barik et al[5] have discussed the chemical reaction effect on peristaltic motion of micropolar fluid through a porous medium with heat absorption in the presence of magnetic field. Precious Sibanda et al [38] have investigated flow of a micropolar fluid in channel with heat and mass transfer. Nayak [37] has discussed steady free convection heat and mass transfer MHD flow of a radiative micropolar fluid in a vertical porous channel with heat source and chemical reaction. Krishna Kumari, et al[26] have discussed the peristaltic motion of a micropolar fluid under the effect of a magnetic field in an inclined channel. Hemadri Reddy et al [24] have analysed peristaltic pumping of a micropolar fluid in an inclined channel with gravity effects. Sreenadh et al [39] have discussed peristaltic flow of micropolar fluid in an asymmetric channel with permeable walls under long wave length and low reynolds number assumptions. Kavitha, et al [25] have discussed the peristaltic flow of a micropolar fluid in a vertical channel with long wave length approximation. Sushil Kumar Ghosh [42] has analysed micropolar fluid flow through a channe with reference to A Mathematical Model Lung Alveolar sheet Asma Kald et al[3] have discussed the conjugate transfer of heat and mass in unsteady flow of a micropolar fluid with wall couple stress. Nabil T. M. Eldabe et al [34] have investigated the peristaltic transport of micropolar fluid through porous medium in a symmetric channel with heat and mass transfer in the presence of generation and radiation.

Flow of fluids with internal heat sources/sins are of great practical as well as theoretical interest. The fluid motion develops slowly due to the development of non-uniformity in the temperature field. The volumetric heat generation/absorption term exerts strong influence on the flow and heat transfer with appreciably large temperature difference. The analysis of temperature as modified by the heat source/sink in moving fluid is important in view of chemical reaction and problem concerned with dissociated fluids. Thermal radiation factor is better suitable for cooling process. The effect of radiation and viscoys dissipation on stagnation-point flow of a micropolar fluid over a non-linearly stretching surface with suction/injection wad discussed by Babu et al [4]. In many chemical engineering processes chemical reaction occurs between a foreign mass and the working fluid which moves due to stretching or otherwise of a surface. The effect of chemical reaction on a moving isothermal vertical surface was studied by Muthucumaraswamy [33].

2. FORMULATION OF THE PROBLEM:

We analyse the motion of an electrically conducting, incompressible micropolar fluid in a two-dimensional vertical porous channel induced by sinusoidal waves propagating with constant speed 'c' along the channel walls. For simplicity, we restrict our discussion to the half width of the channel. We assume that a uniform magnetic field of strength Bo is applied normal to the walls as shown in the figure.1 assuming the magnetic Reynolds to be small we neglect the induced magnetic field.

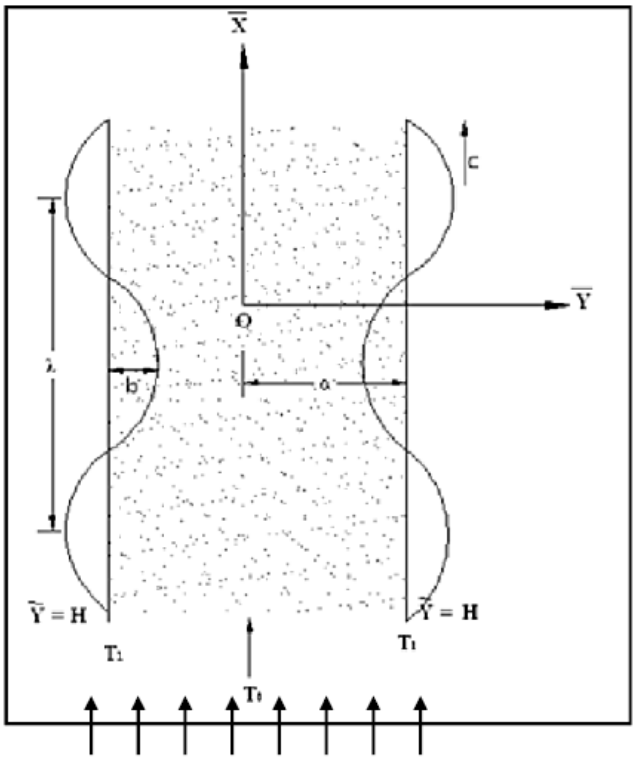

Figure .1 Physical model

The governing equations of flow, heat and mass transfer under Boussinesq approximation are

Continuity equation:

$$\frac{\partial \rho}{\partial t} + \nabla.(\rho \bar{V}) = 0$$

Conservation of linear momentum

$$\rho \bar{V} = (\lambda_\nu + 2\mu_\nu + k_\nu)\nabla(\nabla.\bar{V}) - (\mu_\nu + k_\nu)\nabla x(\nabla x\bar{V}) + k_\nu \nabla x\bar{\omega} - \nabla p - \frac{(\mu + k_\nu)}{k_1}\bar{V} - \rho\bar{g}$$

Conservation of angular momentum

$$\rho\, j\, \bar{\omega} = (\alpha_r + \beta_r + \gamma_r)\nabla\nabla..\bar{\omega} - \gamma_r \nabla x\nabla x\bar{\omega} + k_\nu \nabla x\bar{V} - 2k_\nu\bar{\omega} + \rho l + \bar{J}x\vec{B}$$

Heat equation

$$\rho C_p \frac{dT}{dt} = k_f \nabla^2 T - Q(T - T_o) - \nabla.q_r$$

Concentration equation

$$\frac{dC}{dt} = D_m \nabla^2 C + \frac{D_m K_T}{T_m}\nabla^2 T - k_r C$$

Equation of State

$$\rho - \rho_o = -\beta_T (T - T_o) - \beta_C (C - C_o)$$

Ohm's law can be written as

$$\vec{J} = \sigma(\vec{E} + \vec{V} x \vec{B})$$

Where $\vec{V}$ is the velocity vector of the fluid , $\vec{\omega}$ =(0,0, ω) is the microrotation vector, k is the permeability of porous medium, l is the body couple, ρ is the the fluid density, j is the microinertia parameter, T ,To are the fluid temperature and reference temperature, C, Co are the fluid concentration and reference concentration, k_f is the thermal conductivity, Q is the heat generation, Dm is the molecular diffusivity, K_T is the thermal diffusion ratio, Tm is the mean fluid temperature , J is the current density vector, B is the magnetic induction vector, E is the electric field vector,σ is electric al conductivity, μ_e is the magnetic permeability, μ is the dynamic viscosity, kr is coefficient of chemical reaction, $\alpha_r, \beta_r, \gamma_r, k_\nu, \mu_\nu, \lambda_\nu$ are material parameters(Erigen,1966)(different viscosities that characterize the isotropic properties of the fluid),satisfy

$$2\mu_\nu + k_\nu \geq 0, k_\nu \geq 0, 3\alpha_\nu + \beta_\nu + \gamma_\nu \geq 0, \gamma_\nu \geq \beta_\nu$$

3. SOLUTION OF THE PROBLEM:

We consider the micropolar fluid moving in two-dimensions of Cartesian coordinates(X,Y),where X-axis is taken in motion direction while Y-axis is perpendicular on it and (U,V) are the velocity components in X and Y directions respectively as shown in figure.1.Neglecting body couple, with solenoidal microrotation vector ,then the previous equation runder Boussinesq approximation reduces to

$$\frac{\partial U}{\partial X} + \frac{\partial V}{\partial Y} = 0$$

$$\rho\left(\frac{\partial U}{\partial t} + U\frac{\partial U}{\partial X} + V\frac{\partial U}{\partial Y}\right) = (\mu_\nu + k_\nu)\nabla^2 U + k_\nu \frac{\partial \omega}{\partial Y} - \frac{\partial P}{\partial X} - \left(\frac{(\mu_\nu + k_\nu)}{k}\right)U + \beta_T (T - T_o) + \beta_C (C - C_o) - (\sigma B_o^2)U$$

$$\rho\left(\frac{\partial V}{\partial t} + U\frac{\partial V}{\partial X} + V\frac{\partial V}{\partial Y}\right) = (\mu_\nu + k_\nu)\nabla^2 V + k_\nu \frac{\partial \omega}{\partial X} - \frac{\partial P}{\partial Y} - \left(\frac{(\mu_\nu + k_\nu)}{k}\right)V$$

$$\rho C_p\left(\frac{\partial T}{\partial t} + U\frac{\partial T}{\partial X} + V\frac{\partial T}{\partial Y}\right) = k_f \nabla^2 T - \frac{\partial q_r}{\partial Y} - Q(T - T_o)$$

$$\left(\frac{\partial C}{\partial t} + U\frac{\partial C}{\partial X} + V\frac{\partial C}{\partial Y}\right) = D_m \nabla^2 C + \frac{D_m K_T}{T_m}\nabla^2 T - k_r C$$

Using Rosseland approximation we have

$$q_r = -\frac{4\sigma^\bullet}{3\beta_R}\frac{\partial T'^4}{\partial Y}$$

Where $\sigma^\bullet$ is the Stefan-Boltzmann constant, β_R is mean absorption coefficient (Mahmoud and Waheed [27])

The geometry of the wall surface is defined as

$$Y = H = d + bCos\left(\frac{2\pi}{\lambda}(X - Ct)\right)$$

Where d is is the half-width of the channel, b is the wave amplitude , λ is the wavelength ,c is the velocity propagation, and t is the time.

The appropriate boundary conditions are

$$\psi = 0, \frac{\partial^2 \psi}{\partial Y^2} = 0, \omega = 0, T = T_0, C = C_0 \quad \text{On Y=0}$$

$$\psi = q, \omega = 0, \frac{\partial \psi}{\partial Y} = 0, T = T_w, C = C_w \quad \text{On Y=H}$$

Where ψ is the stream function ($U = \frac{\partial \psi}{\partial Y}, V = -\frac{\partial \psi}{\partial X}$), q is the flux of flow.

Introducing a wave frame (x, y) moving with the velocity c away from the laboratory frame (X, Y), by the transformations

$$x = X - ct, y = Y, u = U - c, v - V, p(x) = P(X, t) \tag{17}$$

Where u and v are the fluid velocity components and P is pressure in the wave frame of references.

Introducing the following non-dimensional variables

$$\vec{x} = \frac{x}{\lambda}, \bar{y} = \frac{y}{d}, \vec{u} = \frac{u}{c}, \bar{v} = \frac{v}{c\delta}, h = \frac{H}{d}, \delta = \frac{d}{\lambda}, \vec{\psi} = \frac{\psi}{cd}, \bar{p} = \frac{d^2}{\mu}\frac{p}{\lambda c},$$

$$\mathrm{Re} = \frac{\rho c d}{\mu}, \bar{j} = \frac{j}{d^2}, \omega = \frac{\omega d}{c}, k = \frac{d^2}{K^2}, \theta = \frac{T - T_o}{T_w - T_o}, \phi = \frac{C - C_o}{C_w - C_o} \tag{18}$$

Using the transformation (17) and non-dimensional variables (18), after drop-ping the bars and under the assumptions of long wavelength approximations

(δ <1) and low Reynolds number (Re) ,the equations 7-12 reduce to

$$\frac{\partial p}{\partial x} = \left(\frac{1}{1-N}\right)\frac{\partial^2 u}{\partial y^2} + \left(\frac{N}{1-N}\right)\frac{\partial \omega}{\partial y} - \left(M^2 + \frac{1}{K}\right)\left(\frac{1}{(1-N)}\right)(u+1) - G(\theta + N\phi) \tag{19}$$

$$\frac{\partial p}{\partial x} = 0 \tag{20}$$

$$\left(\frac{2-N}{m^2}\right)\frac{\partial^2 \omega}{\partial y^2} - \frac{\partial u}{\partial y} - 2\omega = 0 \tag{21}$$

$$\left(1 + \frac{4Rd}{3}\right)\frac{\partial^2 \theta}{\partial y^2} + \mathrm{Pr} G\theta = 0 \tag{22}$$

$$\frac{\partial^2 \phi}{\partial y^2} + ScSr\frac{\partial^2 \theta}{\partial y^2} - \gamma\phi = 0 \tag{23}$$

The channel wall equation will be

$$y = h = 1 + \varepsilon Cos(2\pi x), \tag{24}$$

Where

$Gr = \frac{\beta g (T_w - T_o) d^2}{\mu}$ (Grashof number); $M^2 = \frac{\sigma B_o^2 d^2}{\mu_e}$ (Magnetic parameter)

$K = \frac{d^2}{k_1^2}$ (Porous parameter); $Nr = \frac{\beta_C (C_w - C_o)}{\beta_T (T_w - T_o)}$ (Buoyancy ratio

$N=\frac{k_\nu}{\mu_\nu+k_\nu}$ (Coupling parameter); $m^2=\frac{k_\nu d^2(2\mu_\nu+k_\nu)}{\lambda_\nu(\mu_\nu+k_\nu)}$ (Micropolar parameter)

$\Pr=\frac{\mu_\nu C_p}{k_f}$ (Prandtl number); $Rd=\frac{4\sigma^{\bullet}T_o^3}{\beta_R k_f}$ (Radiation parameter)

$Q=\frac{Q_H d^2}{\mu_\nu C_P}$ (Heat source parameter); $Sc=\frac{\mu_\nu}{\rho D_m}$ (Schmidt number)

$Sr=\frac{\rho D_m K_T(T_w-T_o)}{\mu_\nu(C_w-C_o)}$ (Soret parameter); $\gamma=\frac{k_r}{d^2}$ (Chemical reaction parameter)

$\varepsilon=\frac{b}{d}$ <1(Amplitude ratio)

Using equation (20) in (19), the governing equations in terms of stream function reduce to

$$\frac{\partial^4\psi}{\partial y^4}+N\frac{\partial\omega}{\partial y}-(M^2+K^{-1})\frac{\partial^2\psi}{\partial y^2}=-G(\frac{\partial\theta}{\partial y}+N\frac{\partial\phi}{\partial y}) \quad (25)$$

$$\frac{\partial^2\psi}{\partial y^2}-(\frac{2-N}{m^2})\frac{\partial^2\omega}{\partial y^2}+2\omega=0 \quad (26)$$

$$(1+\frac{4Rd}{3})\frac{\partial^2\theta}{\partial y^2}-\Pr Q\theta=0 \quad (27)$$

$$\frac{\partial^2\phi}{\partial y^2}+ScSr\frac{\partial^2\theta}{\partial y^2}-(Sc\gamma)\phi=0 \quad (28)$$

The transformed boundary conditions in terms of stream function are

$$\psi=0,\frac{\partial^2\psi}{\partial y^2}=0,\omega=0,\theta=0,\phi=0 \quad \text{on} \quad y=0 \quad (29)$$

$$\psi=q,\omega=0,\frac{\partial\psi}{\partial y}=-1,\theta=1,\phi=1 \quad \text{On } y=h \quad (30)$$

The solutions of equations (25)-(28) subject to boundary conditions (equations 29-30) are

$$\theta(y)=\frac{Sinh(\beta_1 y)}{Sinh(\beta_1 h)} \quad (31)$$

$$\phi(y)=\frac{Sinh(\beta_1 y)}{Sinh(\beta_1 h)}+A_1(Sinh(\beta_1 y)-Sinh(\beta_1 h)\frac{Sinh(\beta_2 y)}{Sinh(\beta_2 h)}) \quad (32)$$

$$\psi(y)=A_{12}Cosh(m_1 y)+A_{13}Sinh(m_1 y)+A_{14}Cosh(m_2 y)+A_{15}Sinh(m_2 y)+A_8Sinh(\beta_1 y)+A_9Cosh(\beta_2 y)+A_6A_{10}y+A_7A_{11} \quad (33)$$

$$\omega(y)=A_{24}Cosh(\beta_3 y)+A_{25}Sinh(\beta_3 y)+f_1(y)$$

$$f_1(y)=A_{18}Cosh(m_1 y)+A_{19}Sinh(m_1 y)+A_{20}Cosh(m_2 y)+A_{21}Sinh(m_2 y)+A_{22}Cosh(\beta_1 y)+A_{23}Cosh(\beta_2 y) \quad (34)$$

$$u(y)=-A_{28}\frac{dp}{dx}(Cosh(M_1 y)+\frac{Sinh(M_1 y)}{Sinh(M_1 h)}+(1+A_{41}+Cosh(M_1 h))\frac{Sinh(M_1 y)}{Sinh(M_1 h)}-A_{42}\frac{Sinh(M_1 y)}{Sinh(M_1 h)}-A_{41}Cosh(M_1 y)+f_2(y)$$

$$f_2(y) = A_{29}Sinh(\beta_3 y) + A_{30}Cosh(\beta_3 y) + A_{31}Sinh(m_1 y) + A_{32}Cosh(m_1 y) + A_{33}Sinh(m_2 y) + A_{34}Cosh(m_2 y) + A_{35}Sinh(\beta_2 y) + A_{36}Cosh(\beta_2 y) + A_{37}Sinh(\beta_1 y) + A_{38}Sinh(\beta_2 y) \quad (35)$$

The volume flux Q through each cross section in the wave form is give by

$$Q = \int_o^h u dy$$

$$= -A_{28}A_{43}(\frac{\partial p}{\partial x}) + A_{44} + A_{45} \quad (36)$$

The pressure gradient is obtained from the equation (36)

$$\frac{\partial p}{\partial x} = \frac{(Q - A_{44} - A_{45})}{A_{28}A_{43}} \quad (37)$$

The time averaged flow rate is

$$\overline{Q} = Q + 1$$

Pumping characteristics:

Integrating the equation (37) with respect to over one wave length, we get the pressure rise (drop)

$$\Delta p = \int_o^1 (\frac{\partial p}{\partial x})$$

The dimensionless friction force F at the wall across one wavelength in channel is given by

$$F = \int_0^1 h(-\frac{\partial p}{\partial x})dx \quad (38)$$

RESLUTS AND DISCUSSION

In the present study, the problem of peristaltic transport of micropolar fluid under the effects of heat generation and radiation with heat and mass transfer through a symmetric channel is modelled mathematically. The governed equations of this problem are formed in two dimensions and transformed from a laboratory frame to a fixed frame, the yield equations written in dimensionless form. The analytical solutions of these equations have been obtained under the conditions of low Reynolds number and long wave length, subject to a set of appropriate boundary conditions using the Mathematica Program. The expressions of velocity profile, microrotation velocity, temperature and concentration distributions have been evaluated for different physical parameters of the problem and have been shown graphically through a set of figures. In our figures we chose *y* between 0 and 1.5 we observed that in the region $0 \leq y \leq 8.0$.

Figs.2a&2b represent the variation of velocity (u) and microrotation (g) with Grashof number Gr. It can be seen from the profiles that an increase in Grashof number leads to a depreciation in velocity and micro-rotation with maximum attained at $\eta=0$.

Figs.3a&3b show the variation of velocity and micro-rotation with magnetic parameter (M). The effect of Hartmann number is to reduce the velocity distribution in the boundary layer which results in thinning in the boundary layer thickness. The decrease in the velocity profile is due to the fact that the transverse magnetic field has a tendency to retard the motion of the fluid as Hartmann number increases the Lorentz force. Also an increase in M reduces the micro-rotation in the flow region.

Fig.4a shows the variation of velocity with inverse Darcy parameter D^{-1}. It is observed from the figure that the velocity distribution deceases with increasing inverse Darcy parameter D^{-1}.This is due to the increase in the obstruction of the fluid motion with increase in the inverse Darcy parameter.(since permeability of the porous medium appears in the denominator of the inverse Darcy parameter), thereby increase in D^{-1} indicates decrease in the permeability of the porous medium so the fluid velocity decreases.Fig.4b exhibits the variation of g with $D^{-1}M$ from the profiles we notice a reduction in g with increase in D^{-1}.

Fig.5a&5b depicts the variation of u &g with Buoyancy ratio (N).It can be seen from the profiles that when the molecular buoyancy force dominates over the thermal buoyancy force the velocity enhances when the buoyancy forces are in the same direction and for the forces acting in opposite directions the velocity reduces in the flow region. Also the micro-rotation (g) increases with N>0 and reduces with N<0(fig.5b)

Figs.6a&6b depict the variation of velocity and microrotation with micropolar parameter (N).It can be seen from the profiles that an increase in N leads to an enhancement in f ‘ and g in the entire flow region. This may be attributed to the fact that an increase in N increases the thickness of the momentum boundary layer.

Figs.7a&7b illustrate the variation of velocity and microrotation with micropolar parameter (β).From fig.6a we notice an enhancement in the velocity with increase in β≤0.4 and for further higher β≥0.6, the velocity depreciates in the flow region. The microrotation (g) reduces with increase in β(fig.7b).

Figs.8a-8c show the variation of u, g and ϕ with thermal radiation parameter (Rd). It can be observed from the profiles that higher the thermal radiation larger the velocity, microrotation and temperature and smaller the concentration in the flow region. This may be attributed to the fact that an increase in Rd leads to an increment in the thickness of the momentum and thermal boundary layers and thinning of the solutal boundary layer.

The effect of heat sources on the velocity, microrotation, temperature and concentration can be seen from figs.9a-9d.from the profiles we find that the presence of the heat generating/absorbed sources heat is absorbed in the boundary layer, which results in the depreciation of velocity, microrotation. An increase in Q>0, reduces the temperature and enhances the concentration while a reversed effect is noticed in the case of increasing Q<0.

Figs.10a-10c represent the variation of velocity, microrotation and concentration with increases in Schmidt number(Sc).from the profiles we find that lesser the molecular diffusivity larger the velocity, microrotation and concentration. This is due to the fact that the thickness of the momentum boundary layer and solutal boundary layer reduces with increase in Schmidt number.

Figs.11a-11c represents velocity, microrotation and concentration with chemical reaction parameter (γ).It can be observed from the profiles that the velocity, microratation and concentration reduce in the degenerating chemical reaction case while they experience an enhancement in the generating chemical reaction case.

The effect of thermo-diffusion (Sr) on velocity, microrotation and concentration can be seen from figs.12a-12c.It can be observed from the profiles that higher the thermo-diffusion effects larger the thickness of the momentum boundary layer, microrotation boundary layer and solutal layer which results in an increment in the velocity, microrotation and concentration in the flow region.

The variation of pressure rise Δp for time average flow rate for different values of G is shown in fig.13 it is observed that for a given $\overline{Q}$, Δp decreases as G increases in the co-pumping and free pumping region while it increases in the pumping region. Also for a given Δp ,the flux $\overline{Q}$ decreases with increases in G.

Fig.14 shows the variation of Δp with for different values of magnetic parameter (M).It can be seen from the profiles for a given $\overline{Q}$, Δp increases with increase in magnetic parameter M in both pumping and co-pumping regions. Also for a given Δp ,the flux $\overline{Q}$ increases with increase in M.

Fig.15 illustrates the variation of Δp with $\overline{Q}$ for different values of porous parameter (K).We find from the profiles that for a given $\overline{Q}$, Δp increases with increase in K. Also for a given Δp , $\overline{Q}$ enhances with K.

Fig.16 represents Δp with $\overline{Q}$ for different values of buoyancy ratio(Nr).It can be seen from the profiles that when the molecular buoyancy force dominates over the thermal buoyancy force ,for a given $\overline{Q}$, Δp increases in all pumping, free pumping and co-pumping regions when the buoyancy forces are in the same directions.Also for a given Δp , $\overline{Q}$ enhances with increase in Nr.

Fig.17 shows the variation of Δp with $\overline{Q}$ for different values of Heat source parameter (Q).It can be seen from the profiles that for a given $\overline{Q}$, Δp increases with increase in the strength of the heat generating source (Q>0) in both pumping and co-pumping regions. In the presence of heat absorbing source, Δp deceases with Q<0 in both pumping and co-pumping regions. Also for a given Δp ,the flux $\overline{Q}$ enhances with increase in Q>0 and reduces with Q<0 for $\overline{Q} \leq 0.42$, reduces for $\overline{Q} \geq 0.43$

Fig.18 depicts Δp with $\overline{Q}$ for different values of radiation parameter (Rd). It can be seen from the profiles that for a given $\overline{Q}$, Δp increases with increase in Rd in the pumping and co-pumping regions. Also for given Δp , $\overline{Q}$ increases with Rd.

Fig.19 represents Δp with $\overline{Q}$ for different values of Sc.It is found that for given $\overline{Q}$,the pressure rise increases with increase in Sc in pumping region and reduces in co-pumping region. Also for a given Δp , $\overline{Q}$ increases with Sc.

Fig.20 shows the variation of Δp with $\overline{Q}$ for different values of Soret parameter (Sr).From the profiles we find that for a given $\overline{Q}$, Δp increases with Sr in pumping region and decreases win co-pumping region .Also for a given Δp , $\overline{Q}$ enhances with Sr.

Fig.21 represents Δp with $\overline{Q}$ for different values of chemical reaction parameter (γ).From the profiles we notice that for a given $\overline{Q}$, Δp increases in degenerating chemical reaction case in pumping

region and reduces in co-pumping region. In the generating case, Δp reduces in pumping region and enhances in co-pumping region. Also for a given Δp , $\overline{Q}$ increases with $\gamma>0$ and reduces with $\gamma<0$.

The effect of coupling parameter (N) on the pumping characteristics is exhibited in fig.22.We observe from the profiles that higher the coupling parameter N larger the pressure rise against which pumping works. For a given $\overline{Q}$, the pressure difference increases with increase in N in both pumping and co-pumping regions. Also, for a given Δp , $\overline{Q}$ increases with increase in N.

Fig.23 shows the variation of Δp with $\overline{Q}$ for different values of amplitude ratio (m).It can be seen from the profiles that higher the amplitude ratio (m) smaller the pressure drop in pumping and co-pumping regions. Also for a given Δp , the flux $\overline{Q}$ reduces with increase in amplitude ratio (m).

Figs.24-34 represent the frictional force (F) with time average flux ($\overline{Q}$) for different values of G,M,K,Nr,Rd,Q,Sc,Sr,γ.it can be seen from fig.24 that for a given $\overline{Q}$,the frictional force increases with increase in Grashof number(G).The frictional force enhances with increase in magnetic parameter and porous parameter(fig.25&26).An increase in buoyancy ratio(Nr) increases the frictional force when the buoyancy forces are in the same direction.(fig.27).From fig.28,we notice that ,F increases with increase in the strength of the heat generating source and reduces with that of heat absorbing source. An increases in Rd or Sc or Sr results in an enhancement in F fixing $\overline{Q}$ (figs.29,30&31).The frictional force reduces in the degenerating chemical reaction case and enhances in the generating case(fig.32).From figs.33&34 we observe that the frictional force enhances with coupling parameter(N) and reduces with that of amplitude ratio(m).

Figs.35-37 show the variation of rate of heat transfer (Nu) with Q, Rd and Pr. From the profiles we find that the rate of heat transfer reduces with increase in the strength of the heat generating source and in the case of heat absorbing source, it experiences an enhancement. Higher the radiative heat flux ($Rd\leq1.5$) larger the rate of heat transfer and for still higher $Rd\geq3.5$, Nu reduces. Also lesser the thermal diffusivity, larger the rate of heat transfer (fig.37).

The rate of mass transfer (Sherwood number) is exhibited in figs.38-43 for different variations of Sc,γSr,Q,Rd,Pr.From fig.38 we notice a depreciation in Sh with increase in Sc. The rate of mass transfer reduces in the degenerating chemical reaction case and enhances in the generating chemical reaction case (fig.39).Higher the thermo-diffusion effects lager Sh on the wall (fig.40).An increase in the strength of the heart generating/absorbing source smaller the rate of mass transfer on the wall (fig.41).The rate of mass transfer enhances with increase in Rd and reduces with that of Prandtl number (Pr) (figs.42&43).

COMPARISON

In the absence convective heat and mass transfer (Gr=0, N=0) the results are good agreement with Nabil et al [34].

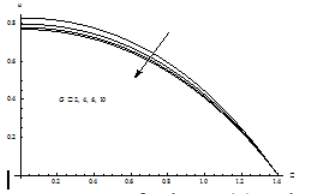

Fig.2a Variation of velocity (u) with Gr
M=0.5, D^{-1} =0.2, N=0.2,β=0.2,Nr=0.5,
Sc=1.3, Sr=0.5, Rd=0.5, Pr=0.71,

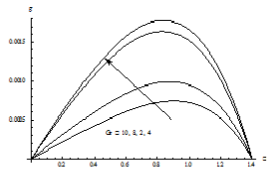

Fig.2b Variation of microrotation (g) with Gr
M=0.5,D^{-1}=\0.2,N=0.2,β=0.2,Nr=0.5,
Sc=1.3, Sr=0.5, Rd=0.5, Pr=0.71,

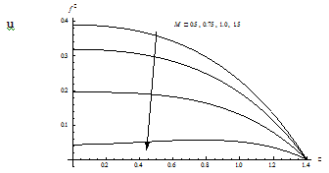

Fig.3a Variation of velocity (u) with M
Gr=2.0, D^{-1} =0.2, N=0.2,β=0.2,Nr=0.5,
Sc=1.3, Sr=0.5, Rd=0.5, Pr=0.71,

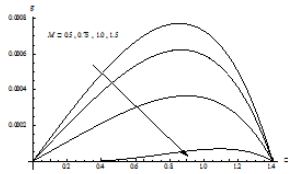

Fig.3b Variation of g with M
D^{-1}=0.2, Gr=2.0, N=0.2,β=0.2,Nr=0.5,
Sc=1.3, Sr=0.5, Rd=0.5, Pr=0.71,

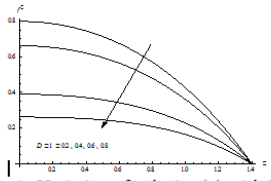

Fig.4a Variation of velocity (u) with D^{-1}
M=0.5, Gr=2.0, N=0.2,β=0.2,Nr=0.5,
Sc=1.3, Sr=0.5, Rd=0.5, Pr=0.71,

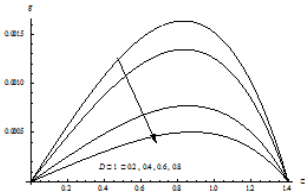

Fig.4b Variation of (g) with D^{-1}
M=0.5, Gr=2.0, N=0.2,β=0.2,Nr=0.5,
Sc=1.3, Sr=0.5, Rd=0.5, Pr=0.71,

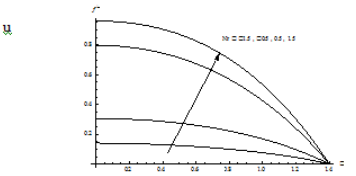

Fig.5a Variation of velocity (u) with Nr
M=0.5, Gr=2.0, N=0.2,β=0.2,Gr=2.0,
Sc=1.3, Sr=0.5, Rd=0.5, Pr=0.71,

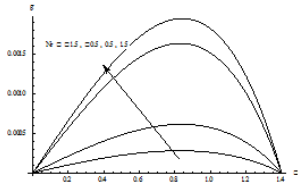

Fig.5b Variation of (g) with Nr
M=0.5, Gr=2.0, N=0.2,β=0.2,Gr=2.0,
Sc=1.3, Sr=0.5, Rd=0.5, Pr=0.71,

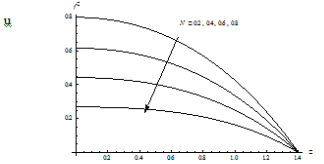

Fig.6a Variation of velocity(u) with N
M=0.5,Gr=2.0,Gr=2.0,β=0.2,Nr=0.5,
Sc=1.3,Sr=0.5,Rd=0.5,Pr=0.71,

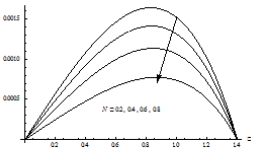

Fig.6b Variation of (g) with N
M=0.5,Gr=2.0,Gr=2.0,β=0.2,Nr=0.5,
Sc=1.3,Sr=0.5,Rd=0.5,Pr=0.71,

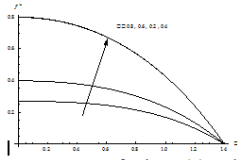

Fig.7a Variation of velocity(u) with β
M=0.5,Gr=2.0,N=0.2,Gr=2.0,Nr=0.5,
Sc=1.3,Sr=0.5,Rd=0.5,Pr=0.71,

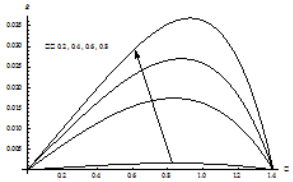

Fig.7b Variation of (g) with β
M=0.5,Gr=2.0,N=0.2,Gr=2.0,Nr=0.5,
Sc=1.3,Sr=0.5,Rd=0.5,Pr=0.71,

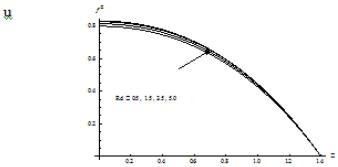

Fig.8a Variation of velocity(u) with Rd
M=0.5,Gr=2.0,N=0.2,β=0.2,Nr=0.5,
Sc=1.3,Sr=0.5,Gr=2.0,Pr=0.71,

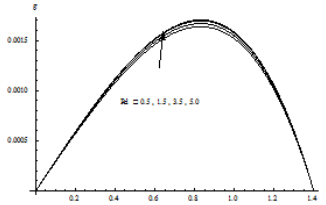

Fig.8b Variation of (g) with Rd
M=0.5,Gr=2.0,N=0.2,β=0.2,Nr=0.5,
Sc=1.3,Sr=0.5,Gr=2.0,Pr=0.71,

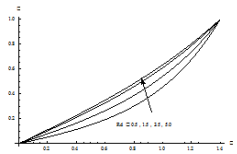

Fig.8c Variation of temperature(θ) with Rd
M=0.5,Gr=2.0,N=0.2,β=0.2,Nr=0.5,
Sc=1.3,Sr=0.5,Gr=2.0,Pr=0.71,

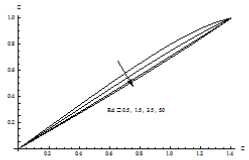

Fig.8d Variation of Concentration(ϕ) with Rd
M=0.5,Gr=2.0,N=0.2,β=0.2,Nr=0.5,
Sc=1.3,Sr=0.5,Gr=2.0,Pr=0.71,

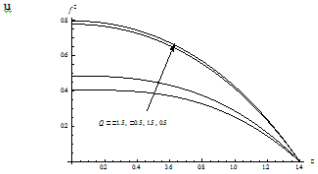

Fig.9a Variation of velocity(u) with Q
M=0.5,Gr=2.0,N=0.2,β=0.2,Nr=0.5,
Sc=1.3,Sr=0.5,Rd=0.5,Pr=0.71

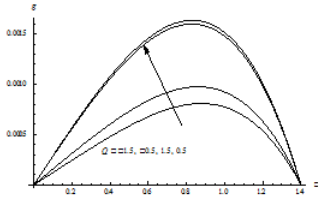

Fig.9b Variation of (g) with Q
M=0.5,Gr=2.0,N=0.2,β=0.2,Nr=0.5,
Sc=1.3,Sr=0.5,Rd=0.5,Pr=0.71

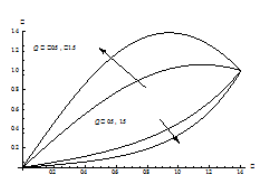

Fig.9c Variation of temperature (θ) with Q
M=0.5, Gr=2.0,N=0.2,β=0.2,Nr=0.5,
Sc=1.3, Sr=0.5, Rd=0.5,Pr=0.71

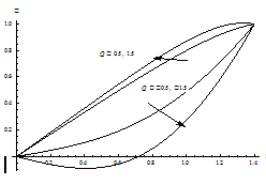

Fig.9d Variation of Concentration(ϕ) with Q
M=0.5,Gr=2.0,N=0.2,β=0.2,Nr=0.5,
Sc=1.3,Sr=0.5,Rd=0.5,Pr=0.71

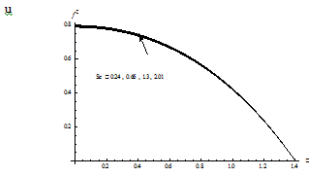

Fig.10a Variation of velocity(u) with Sc
M=0.5,Gr=2.0,N=0.2,β=0.2,Nr=0.5,
Gr=2.0,Sr=0.5,Rd=0.5,Pr=0.71,

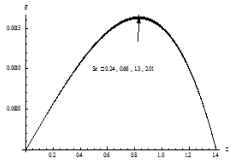

Fig.10b Variation of (g) with Sc
M=0.5,Gr=2.0,N=0.2,β=0.2,Nr=0.5,
Gr=2.0,Sr=0.5,Rd=0.5,Pr=0.71,

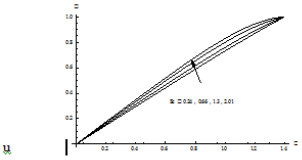

Fig.10c Variation of co0ncentration(ϕ) with Sc
M=0.5,Gr=2.0,N=0.2,β=0.2,Nr=0.5,
Gr=2.0,Sr=0.5,Rd=0.5,Pr=0.71

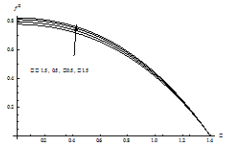

Fig.11a Variation of velocity(u) with γ
M=0.5,Gr=2.0,N=0.2,β=0.2,Nr=0.5,
Sc=1.3,Sr=0.5,Rd=0.5,Pr=0.71,

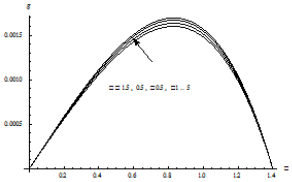

Fig.11b Variation of (g) with γ
M=0.5,Gr=2.0,N=0.2,β=0.2,Nr=0.5,
Sc=1.3,Sr=0.5,Rd=0.5,Pr=0.71,

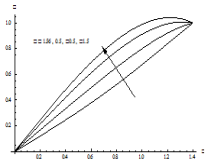

Fig.11c Variation of Concentration(ϕ) with γ
M=0.5,Gr=2.0,N=0.2,β=0.2,Nr=0.5,
Sc=1.3,Sr=0.5,Rd=0.5,Pr=0.71

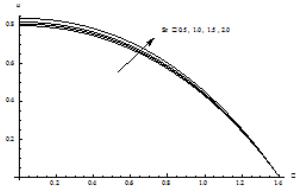

Fig.12a Variation of velocity(u) with Sr
M=0.5,Gr=2.0,N=0.2,β=0.2,Nr=0.5,
Sc=1.3,Gr=2.0,Rd=0.5,Pr=0.71

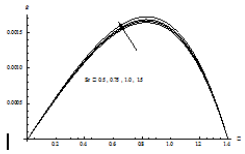

Fig.12b Variation of (g) with Sr
M=0.5,Gr=2.0,N=0.2,β=0.2,Nr=0.5,
Sc=1.3,Gr=2.0,Rd=0.5,Pr=0.71

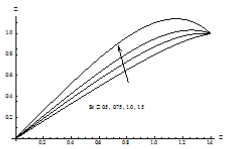

Fig.12c Variation of Concentration (ϕ) with Sr
M=0.5,Gr=2.0,N=0.2,β=0.2,Nr=0.5,
Sc=1.3,Gr=2.0,Rd=0.5,Pr=0.71

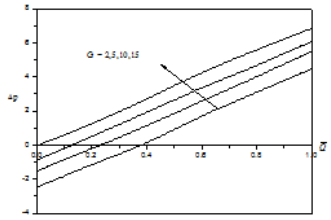

Fig.13 Effect of G on Δp ($\overline{Q}$)
M=0.5, K=0.2, Nr =0.5, Q=2, Rd=0.5,
Sc=1.3, Sr=0.4, γ=0.5,N=0.2, m=2

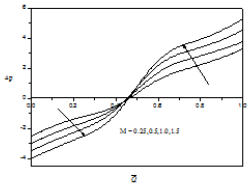

Fig.14 Effect of M on Δp ($\overline{Q}$)
G=2, K=0.2, Nr =0.5, Q=2, Rd=0.5,
Sc=1.3, Sr=0.4, γ=0.5,N=0.2, m=2

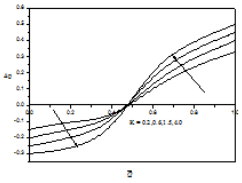

Fig.15 Effect of K on Δp ($\overline{Q}$)
G=2,M=0.5, Nr =0.5, Q=2, Rd=0.5,
Sc=1.3, Sr=0.4, γ=0.5,N=0.2, m=2

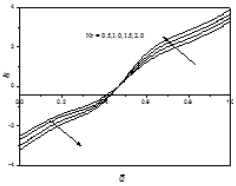

Fig.16 Effect of Nr on Δp ($\overline{Q}$)
G=2,M=0.5, K=0.2, Q=2, Rd=0.5,
Sc=1.3, Sr=0.4, γ=0.5,N=0.2, m=2

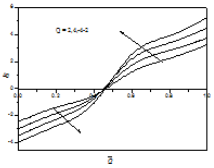

Fig.17 Effect of Q on Δp ($\overline{Q}$)
G=2,M=0.5, K=0.2, Nr =0.5, Rd=0.5,
Sc=1.3, Sr=0.4, γ=0.5,N=0.2, m=2

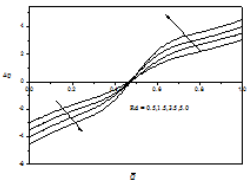

Fig.18 Effect of Rd on Δp ($\overline{Q}$)
G=2,M=0.5, K=0.2, Nr =0.5, Q=2,
Sc=1.3, Sr=0.4, γ=0.5,N=0.2, m=2

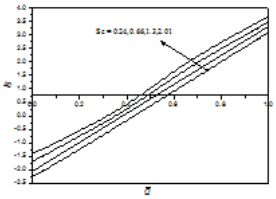

Fig.19 Effect of Sc on Δp ($\overline{Q}$)
G=2,M=0.5, K=0.2, Nr =0.5, Q=2, Rd=0.5,
Sr=0.4, γ=0.5,N=0.2, m=2

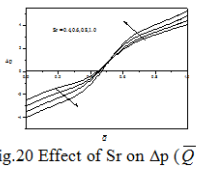

Fig.20 Effect of Sr on Δp ($\overline{Q}$)
G=2,M=0.5, K=0.2, Nr =0.5, Q=2, Rd=0.5,
Sc=1.3, γ=0.5,N=0.2, m=2

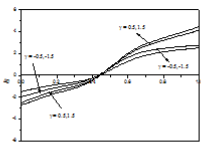

Fig.21 Effect of γ on Δp ($\overline{Q}$)
G=2,M=0.5, K=0.2, Nr =0.5, Q=2, Rd=0.5,
Sc=1.3, Sr=0.4, N=0.2, m=2

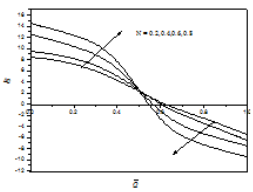

Fig.22 Effect of N on Δp ($\overline{Q}$)
G=2,M=0.5, K=0.2, Nr =0.5, Q=2, Rd=0.5,
Sc=1.3, Sr=0.4, γ=0.5, m=2

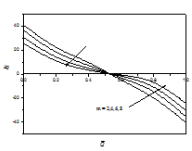

Fig.23 Effect of m on Δp ($\overline{Q}$)
G=2,M=0.5, K=0.2, Nr =0.5, Q=2, Rd=0.5,
Sc=1.3, Sr=0.4, γ=0.5,N=0.2

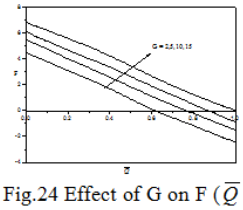

Fig.24 Effect of G on F ($\overline{Q}$)
M=0.5, K=0.2, Nr =0.5, Q=2, Rd=0.5,
Sc=1.3, Sr=0.4, γ=0.5,N=0.2, m=2

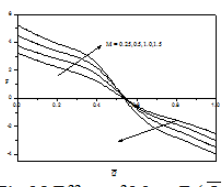

Fig.25 Effect of M on F ($\overline{Q}$)
G=2, K=0.2, Nr =0.5, Q=2, Rd=0.5,
Sc=1.3, Sr=0.4, γ=0.5,N=0.2, m=2

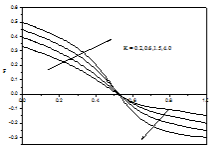

Fig.26 Effect of K on F ($\overline{Q}$)
G=2,M=0.5, Nr =0.5, Q=2, Rd=0.5,
Sc=1.3, Sr=0.4, γ=0.5,N=0.2, m=2

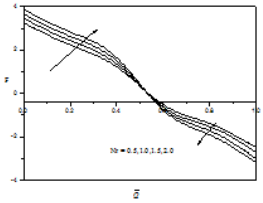

Fig.27 Effect of Nr on F ($\overline{Q}$)
G=2,M=0.5, K=0.2, Q=2, Rd=0.5,
Sc=1.3, Sr=0.4, γ=0.5,N=0.2, m=2

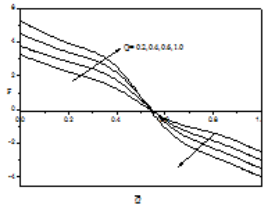

Fig.28 Effect of Q on F ($\overline{Q}$)
G=2,M=0.5, K=0.2, Nr =0.5, Rd=0.5,
Sc=1.3, Sr=0.4, γ=0.5,N=0.2, m=2

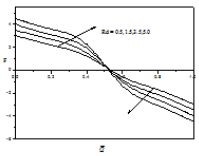

Fig.29 Effect of Rd on F ($\overline{Q}$)
G=2,M=0.5, K=0.2, Nr =0.5, Q=2,
Sc=1.3, Sr=0.4, γ=0.5,N=0.2, m=2

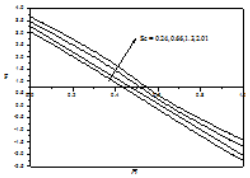

Fig.30 Effect of Sc on F ($\overline{Q}$)
G=2,M=0.5, K=0.2, Nr =0.5, Q=2, Rd=0.5,
Sr=0.4, γ=0.5,N=0.2, m=2

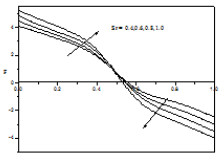

Fig.31 Effect of Sr on F ($\overline{Q}$)
G=2,M=0.5, K=0.2, Nr =0.5, Q=2, Rd=0.5,
Sc=1.3, γ=0.5,N=0.2, m=2

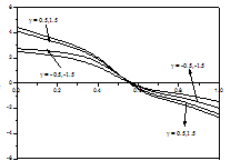

Fig.32 Effect of γ on F ($\overline{Q}$)
G=2,M=0.5, K=0.2, Nr =0.5, Q=2, Rd=0.5,
Sc=1.3, Sr=0.4, N=0.2, m=2

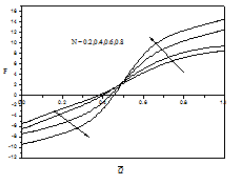

Fig.33 Effect of N on F ($\overline{Q}$)
G=2,M=0.5, K=0.2, Nr =0.5, Q=2, Rd=0.5,
Sc=1.3, Sr=0.4, γ=0.5, m=2

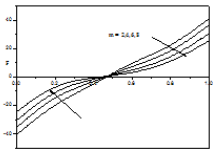

Fig.34 Effect of m on F ($\overline{Q}$)
G=2,M=0.5, K=0.2, Nr =0.5, Q=2, Rd=0.5,
Sc=1.3, Sr=0.4, γ=0.5,N=0.2

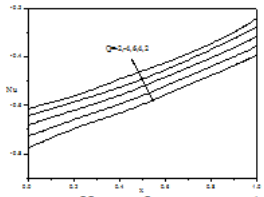

Fig.35 Effect of Q on Nu (x)
Rd=0.5, Pr=0.71

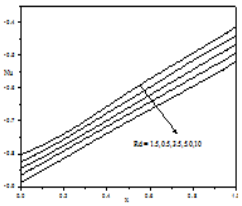

Fig.36 Effect of Rd on Nu (x)
Q=2, Pr=0.71

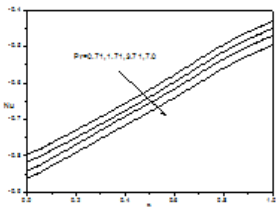

Fig.37 Effect of Pr on Nu (x)
Q=2, Rd=0.5

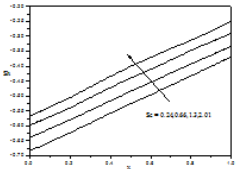

Fig.38 Effect of Sc on Sh (x)
γ=0.5, Sr=0.5, Q=0.5, Rd=0.5, Pr=0.71

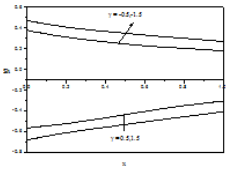

Fig.39 Effect of γ on Sh (x)
Sc = 1.3, Sr=0.5, Q=0.5, Rd=0.5, Pr=0.71

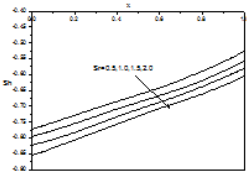

Fig.40 Effect of Sr on Sh (x)
Sc = 1.3, γ=0.5, Q=0.5, Rd=0.5, Pr=0.71

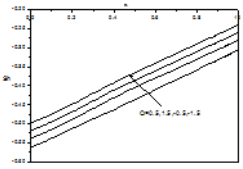

Fig.41 Effect of Q on Sh (x)
Sc = 1.3, γ=0.5, Sr=0.5, Rd=0.5, Pr=0.71

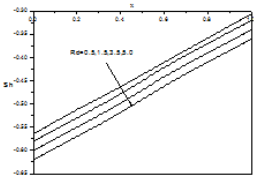

Fig.42 Effect of Rd on Sh (x)
Sc = 1.3, γ=0.5, Sr=0.5, Q=0.5, Pr=0.71

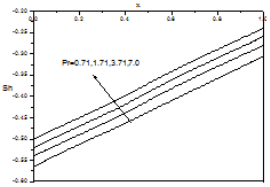

Fig.43 Effect of Pr on Sh (x)
Sc = 1.3, γ=0.5, Sr=0.5, Q=0.5, Rd=0.5

CONCLUSION

The problem of two dimensional peristaltic flow of a micropolar fluid through a symmetric channel with the effects of heat generation and radiation with heat and mass transfer has been investigated. The equations governing the fluid flow, subjected to a set of appropriate boundary conditions, have been solved analytically under the conditions of low Reynolds number and long wave length. The solutions of these equations are obtained as functions of the physical parameters of the problem; the effects of these parameters of the problem on these solutions have been shown graphically.

REFERENCES

1. Abo-Eldahab E, Barakat E, Nowar Kh (2012). Hall currents and heat transfer effects on peristaltic transport in a vertical asymmetric channel through a porous medium. Math. Probl. Eng. pp. 1- 23.
2. Ali N, Hayat T (2008). Peristaltic flow of a micropolar fluid in an asymmetric channel. J. Comput. Math. Appl. 55(4):589-608.
3. Asma Kald,IIyas Khan,Arshad Khan and Sharidan Shafie:Conjugate transfer of heat and mass in unsteady flow of a micropolar fluid with wall couple stress.,AIP Advances,V.5,127125(2015)
4. Babu,M.J,Gupta,R and Sandeep,N:Effect of radiation and viscous dissipation on stagnation-point flow of a micropolar fluid over a nonlinearly stretching surface with suction/injection.,J.Baqsic.Appl.Research Int.,V.7(2),pp.73-82(2015)
5. Barik,R.N and Dash,G.C: Chemical reaction effect on peristaltic motion of micropolar fluid through a porous medium with heat absorption in the presence of magnetic field.,Advances in Applied Science Research,V.6(3)pp.20-34(2015)
6. Bayada G, Banhaoucha N (2008). Wall slip induced by a micropolar fluid. J. Eng. Math. 60:89-100.
7. Devi G, Devanathan R (1975). Peristaltic motion of a micropolar fluid. Proc. Indian Acad. Sci. 81(A):149-163.
8. Eldabe NTM (2001). Heat transfer of MHD Non-Newtonian Casson fluid between two rotating cylinders. Mech. Eng. 5(2):237-24.
9. Eldabe NTM, El-Sayed MF, Ghaly AY, Sayed HM (2008). Mixed convective heat and mass transfer in a Non-Newtonian fluid at a peristaltic surface with temperature-dependent viscosity. Arch. Appl. Mech. 78:599-624.
10. Eldabe NTM, Mohamed MAA (2002). Heat and mass transfer in hydromagnetic flow of the Non-Newtonian fluid with heat source over an accelerating surface through a porous medium. Chaos, Solitons Fractels. 13:907- 917.
11. Eldabe NTM, Mohamed MAA, Hagag MA (2008). MHD flow and heat transfer of micropolar visco-elastic fluid between two parallel porous plats with time varing suction. J. Mech. Cont. Math. Sci. 3:217-233.
12. El-Sayed MF, Eldabe NTM, Ghaly AY, Sayed HM (2011). Effects of chemical reaction, heat and mass transfer on non-Newtonian fluid flow through porous medium in a vertical peristaltic tube. Transp. Porous Med. 89:185-212.
13. El-Shehawey EF, El-Dabe NT, El-ghzey EM, Ebaid A (2006). Peristaltic transport in an asymmetric channel through a porous medium. Appl. Math. Comput. 182:140-150.
14. El-Shehawey EF, Husseny SZA (2000). Effects of porous boundaries on peristaltic transport through a porous medium. Acta Mech. 143:165-177.
15. Eringen AC (1966). Theory of micropolar fluids. J. Math. Mech. 16:1-18.
16. Eytan O, Jaffa AJ, Elad D (2001). Peristaltic flow in a tapered channel: Application to embryo transport within the uterine cavity. Med. Eng. Phys. 23:473-482.
17. Fung YC, Yih CS (1968). Peristaltic transport. J. Appl. Mech. 35:669-675.
18. Gharsseldien ZM (2003). On some problems in biofluidmechanics. PhD. dissertation, Math. Dept., Faculty of Science, Al-Azhar University. Egypt.

19. Gharsseldien ZM, Mekheimer KS, Awad AS (2010). The influence of slippage on trapping and reflux limits with peristalsis through an asymmetric channel. Applied Bionics Biomech. 7(2):95-108.
20. Hayat T, Ali N (2008). Effects of an endoscope on peristaltic flow of a micropolar fluid. Math. Comput. Model. 48:721-733.
21. Nasir Ali and Tasawar Hayat: Peristaltic flow of a micropolar fluid in an asymmetric channel., Computers and Mathematics with Applications., V.55,pp.589-608(2008)
22. Hayat T, Ali N, Abbas Z (2007). Peristaltic flow of micropolar fluid in a channel with different wave forms. Phys. Lett. A. 370:331-344.
23. Hayat T, Hina S (2010). The influence of wall properties on the MHD Peristaltic flow of maxwell fluid with heat and mass transfer. Nonlinear Analysis: Real World Applications. 11:3155-3169.
24. Hemadri Reddy,R,Kavitha,a,sreenadeh,S and Hariprabhakaran,P:Peristaltic pumping of a micropolar fluid in an inclined channel.,Interntional journal of Innovative technology &creative engineering ,V.1(6),pp.22-29(2012)
25. Kavitha.K,Hemandri Reddy.R,Sreenadh.S,saravana.R and srinivas, A.N.S: peristaltic flow of a micropolar fluid in a vertical channel with long wave length approximation., Advances in applied Science Research, V.2(1), pp.269-279 (2011)
26. Krishna Kumari,S.V.H.N and Saroj D Venekar,P and Ravi Kumar,Y.V.K:Peristaltic motion of a micropolar fluid under the effect of a magnetic field in an inclined channel. The international journal of Engineering and science,V.2(2),pp.31-40(2013)
27. Mahmoud MAA, Waheed SE (2012). MHD stagnation point flow of a micropolar fluid towards a moving surface with radiation. Meccanica. 47(5):1119-1130.
28. Mekheimer KS (2003). Nonlinear peristaltic transport through a porous medium in an inclined planar channel. J. Porous Media. 6(3):189-201.
29. Mekheimer KS, Abd Elmaboud Y (2008). The influence of a micropolar fluid on peristaltic transport in an annulus: application of the clot model. Appl.Bionics Biomech. 5(1):13-23.
30. Mishra M, Rao AR (2003). Peristaltic transport of a Newtonian fluid in an asymmetric Channel. Z. angew. Math. Phys. 54:532-550.
31. Muthu P, Ratnish KBV, Chandra P (2003). On the influence of wall properties in the peristaltic motion of micropolar fluid. ANZIAM J. 45:245-260.
32. Muthu P, Ratnish KBV, Chandra P (2008). Peristaltic motion of micropolar fluid in circular cylindrical tubes: Effect of wall properties. Appld. Mathl. Model. 32:2019-2033.
33. Muthucumaeaswamy,R:Effect of a chemical reaction on a moving isothermal vewrtical surface with suction,Acta Mechanica,V.155(1),pp.65-70(2002)
34. Nabil T. M. Eldabe, Afaf S. Zaghrout, Hameda M. Shawky and Amera S. Awad : Peristaltic transport of micropolar fluid through porous medium in a symmetric channel with heat and mass transfer in the presence of generation and radiation, *African Journal of Mathematics and Computer Science Research*, Vol. 6(6), pp. 121-129, June, 2013, DOI: 10.5897/AJMCSR2013.0478 , ISSN 2006-9731 © 2013 Academic Journals http://www.academicjournals.org/AJMCSR

35. Nadeem S, Noreen SA (2009). Influnce of heat transfer on a peristaltic transport of Herschel-Bulkley fluid in a mon-uniform inclined tube. Commun. Nonlinear Sci. Numer. Simulat. 14:4100-4113.
36. Nadeem S, Noreen SA, Bibi N, Ashiq S (2010). Influnce of heat and mass transfer on a peristaltic flow of a third order fluid in a diverging tube. Commun Nonlinear Sci. Numer. Simulat. 15:2916-2931.
37. Nayak,M.K: Steady free convection heat and mass transfer MHD flow of a radiative micropolar fluid in a vertical porous channel with heat source and chemical reaction.,AMSE JOURNALS, Series:Modelling B:V.84,No.2,pp.52-79(2015)
38. Precious Sibanda and Eaiz Ga Awad: Flow of a micropolar fluid in channel with heat and mass transfer.,Latest Trends on Theoretical and Applied Mechanics,Fluid Mechanics and Heat &Mass transfer,ISSN:1792-4359,ISBN:978-960-474-2110-0(2015)
39. Sreenadh.S, Lakshminarayana.P and Sucharitha. G: peristaltic flow of micropolar fluid in an asymmewtric channel with permeable walls.,Int.J.Appl.math and Mech,V,&(20),pp.18-327(2011)
40. Srinivasacharya D, Mishra M, Rao AR (2003). Peristaltic pumping of a micropolar fluid in a tube. Acta. Mech. 161:165-178.
41. Srivastava LM, Srivastava VP (1982). Peristaltic transport of a two-layered model of physiological fluid. J. Biomech. 15(4):257-265.
42. Sushil Kumar Ghosh:Micropolar fluid flow through a channel-A Mathematical Model Lung Alveolar sheet.,journal of physical sciences,V.15,pp.43-57(2011)